Supporting Information for

DBMLFF: Linear scaling machine learning force fields via electron density decomposition for molecular electrolytes

Jie Shen[a], Chenyu Wang[a], Libin Chen[a], Shaoqin Jiang[c,*], Jianhui Chen[a], Cuilian Wen[a], Bo Wu[a], Baisheng Sa[a,*], Lin-Wang Wang[b,*]

[a] *State Key Laboratory of Green and Efficient Development of Phosphorus Resources, Materials Genome Institute, College of Materials Science and Engineering, Fuzhou University, Fuzhou 350108, China.*

[b] *Institute of Semiconductor, Chinese Academy of Science, Beijing, 100083, China*

[c] *LonXun KuangTeng Technology Inc, Beijing, 100083, China*

E-mail addresses:
*bssa@fzu.edu.cn (B. Sa);
*jiangshaoqin@pwmat.com (S. Jiang);
*lwwang@semi.ac.cn (L.-W. Wang)

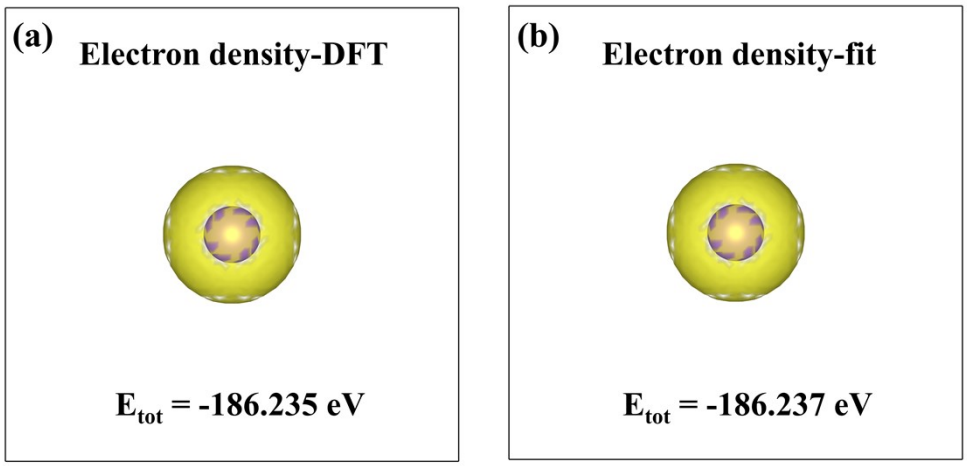

Fig. S1 Isosurface plots and corresponding total energy values of (a) DFT-calculated and (b) spherically-fitted charge density distributions for Li^+ ion with the isosurface value of 0.00001e/bohr^3.

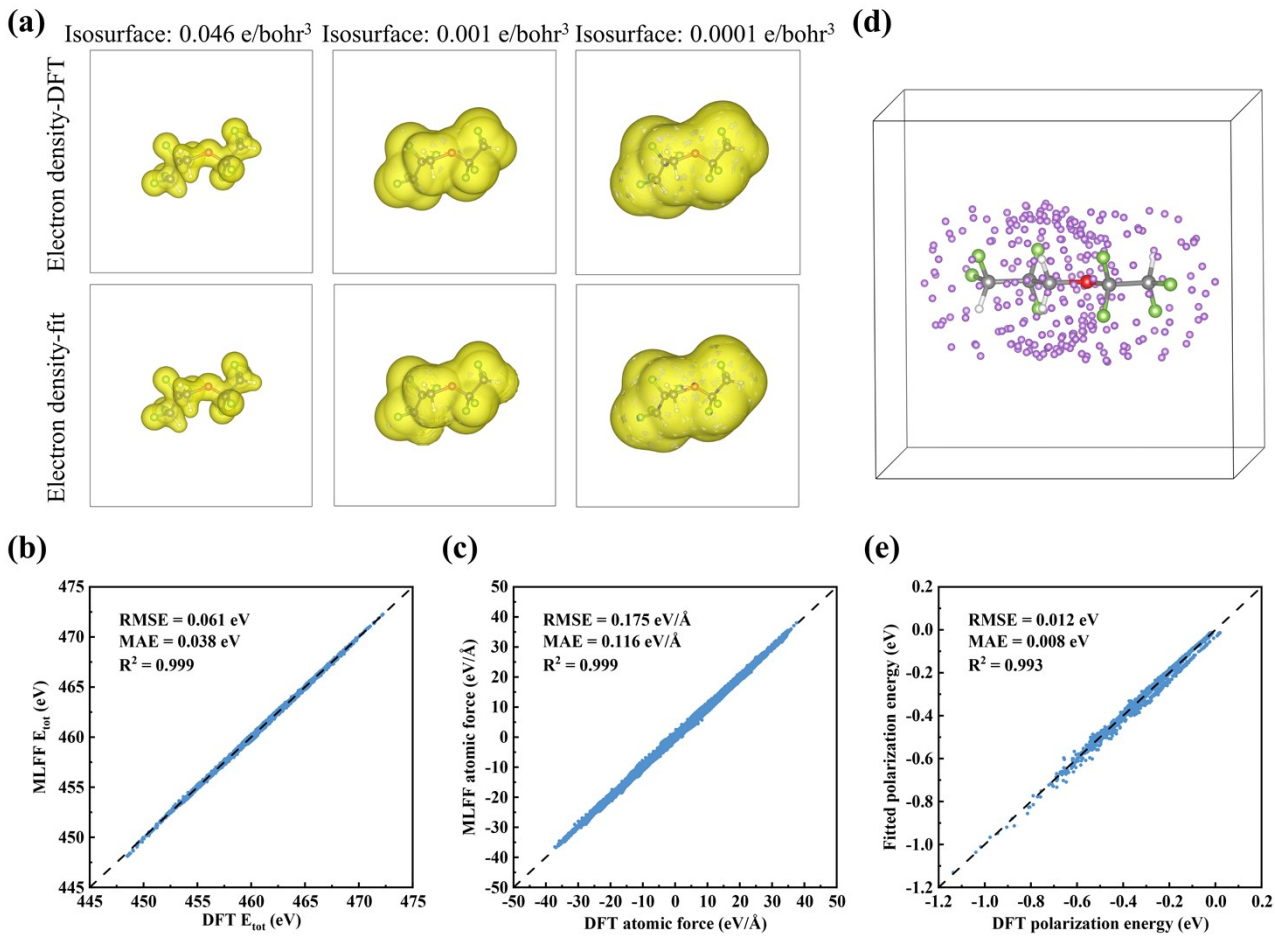

Fig. S2 TTE molecule analysis: (a) DFT-calculated (upper) vs. spherically-fitted (lower) electron density isosurfaces at multiple values; (b) MLFF-predicted total energy and (c) atomic forces across configurations; (d) Probe charge position Rp distribution at a representative probe-molecule distance; (e) Correlation between DFT-calculated and fitted polarization energies under varied probe configurations.

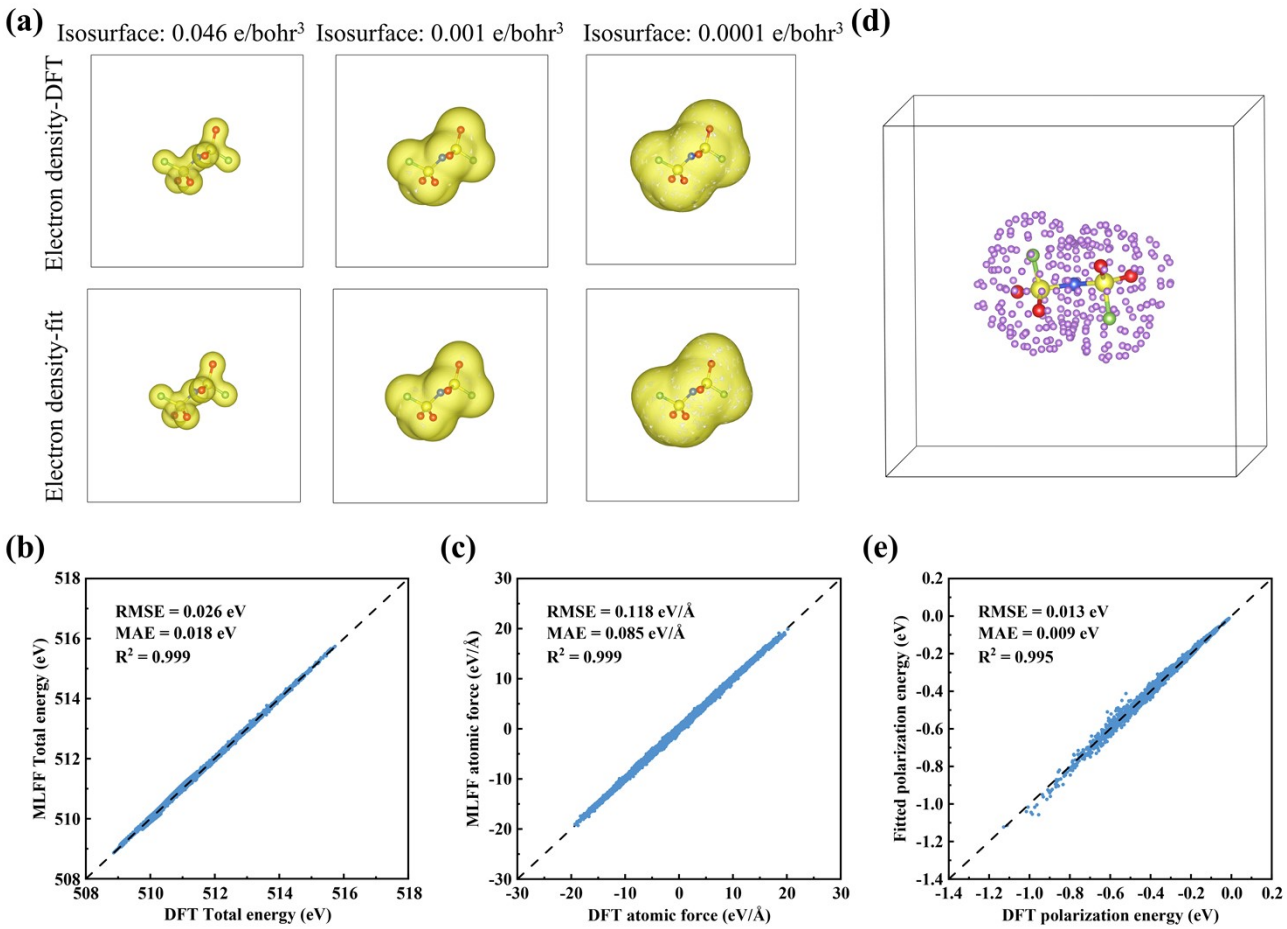

Fig. S3 FSI^- anion analysis: (a) DFT-calculated (upper) vs. spherically-fitted (lower) electron density isosurfaces at multiple values; (b) MLFF-predicted total energy and (c) atomic forces across configurations; (d) Probe charge position Rp distribution at a representative probe-molecule distance; (e) Correlation between DFT-calculated and fitted polarization energies under varied probe configurations.

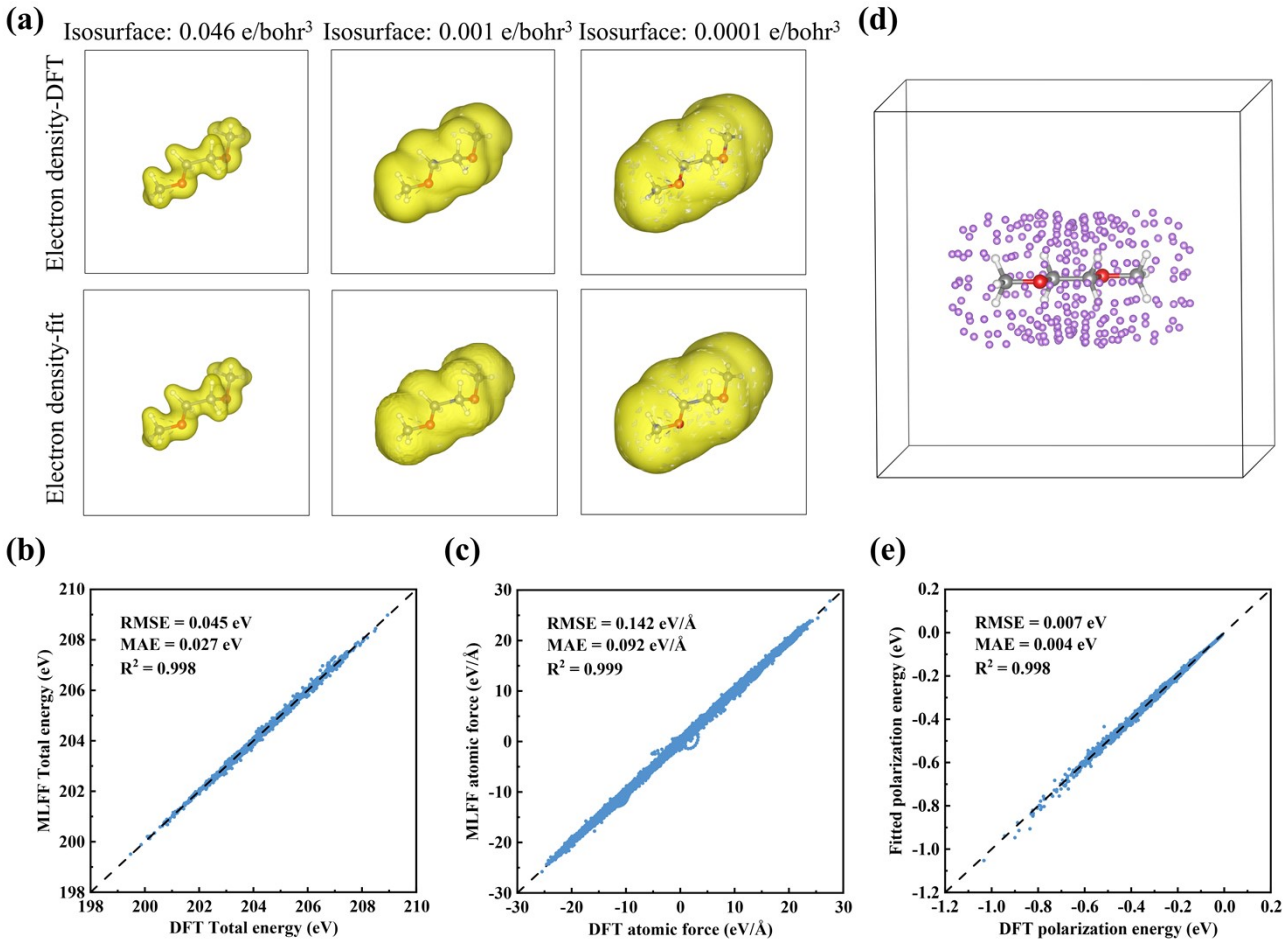

Fig. S4 EGDME molecule analysis: (a) DFT-calculated (upper) vs. spherically-fitted (lower) electron density isosurfaces at multiple values; (b) MLFF-predicted total energy and (c) atomic forces across configurations; (d) Probe charge position Rp distribution at a representative probe-molecule distance; (e) Correlation between DFT-calculated and fitted polarization energies under varied probe configurations.

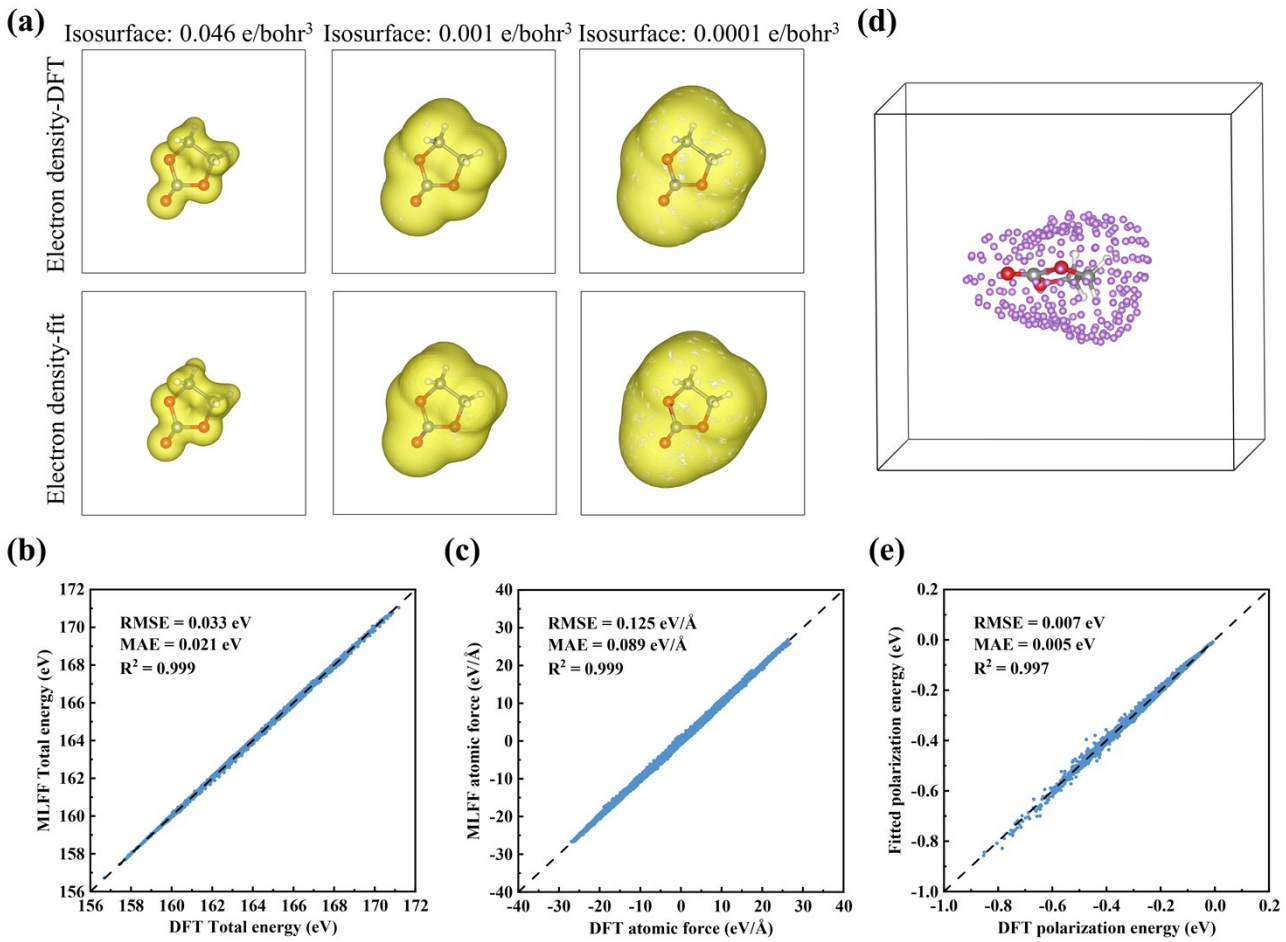

Fig. S5 EC molecule analysis: (a) DFT-calculated (upper) vs. spherically-fitted (lower) electron density isosurfaces at multiple values; (b) MLFF-predicted total energy and (c) atomic forces across configurations; (d) Probe charge position Rp distribution at a representative probe-molecule distance; (e) Correlation between DFT-calculated and fitted polarization energies under varied probe configurations.

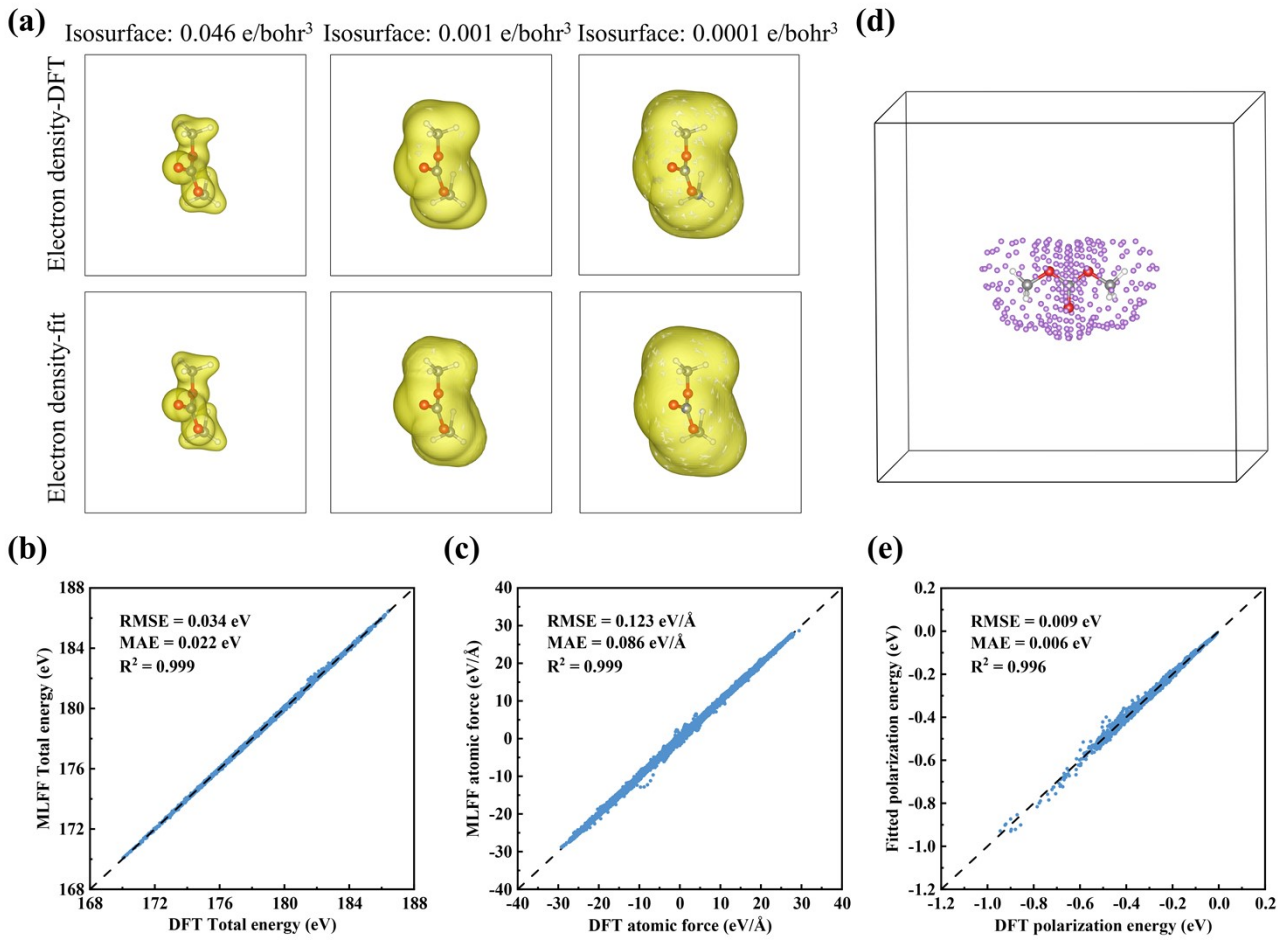

Fig. S6 DMC molecule analysis: (a) DFT-calculated (upper) vs. spherically-fitted (lower) electron density isosurfaces at multiple values; (b) MLFF-predicted total energy and (c) atomic forces across configurations; (d) Probe charge position Rp distribution at a representative probe-molecule distance; (e) Correlation between DFT-calculated and fitted polarization energies under varied probe configurations.

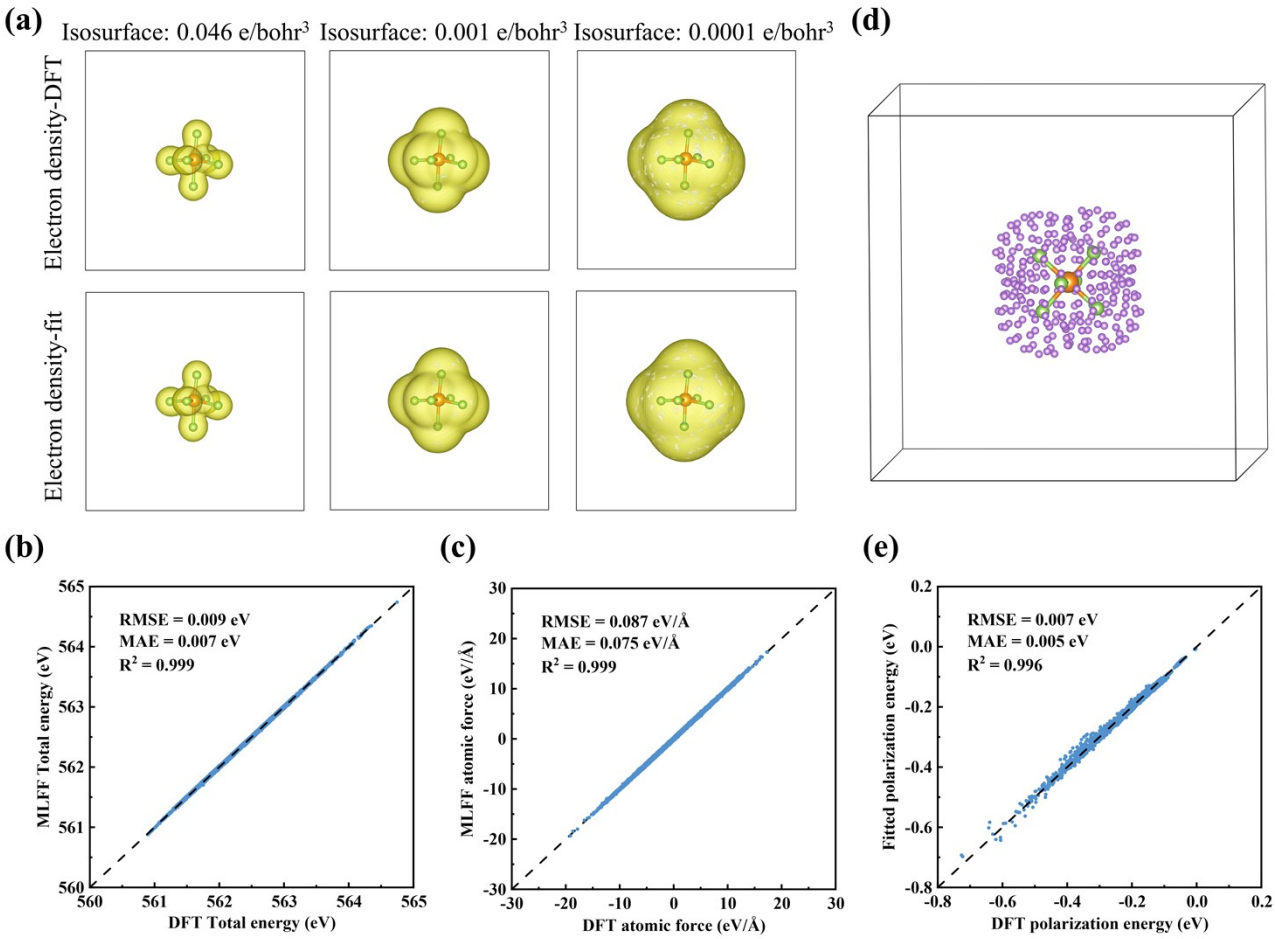

Fig. S7 PF_6^- analysis: (a) DFT-calculated (upper) vs. spherically-fitted (lower) electron density isosurfaces at multiple values; (b) MLFF-predicted total energy and (c) atomic forces across configurations; (d) Probe charge position Rp distribution at a representative probe-molecule distance; (e) Correlation between DFT-calculated and fitted polarization energies under varied probe configurations.

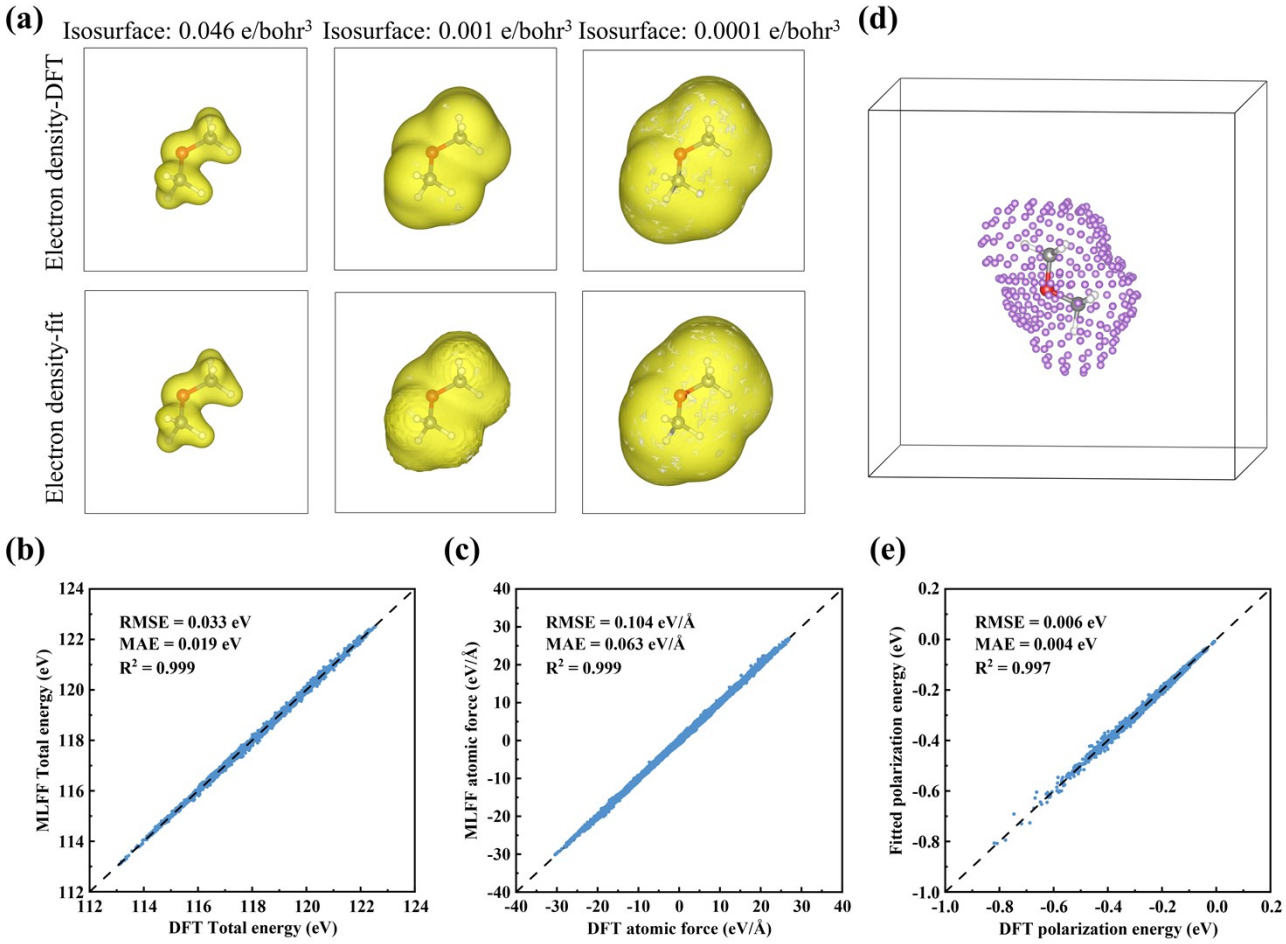

Fig. S8 DME analysis: (a) DFT-calculated (upper) vs. spherically-fitted (lower) electron density isosurfaces at multiple values; (b) MLFF-predicted total energy and (c) atomic forces across configurations; (d) Probe charge position Rp distribution at a representative probe-molecule distance; (e) Correlation between DFT-calculated and fitted polarization energies under varied probe configurations.

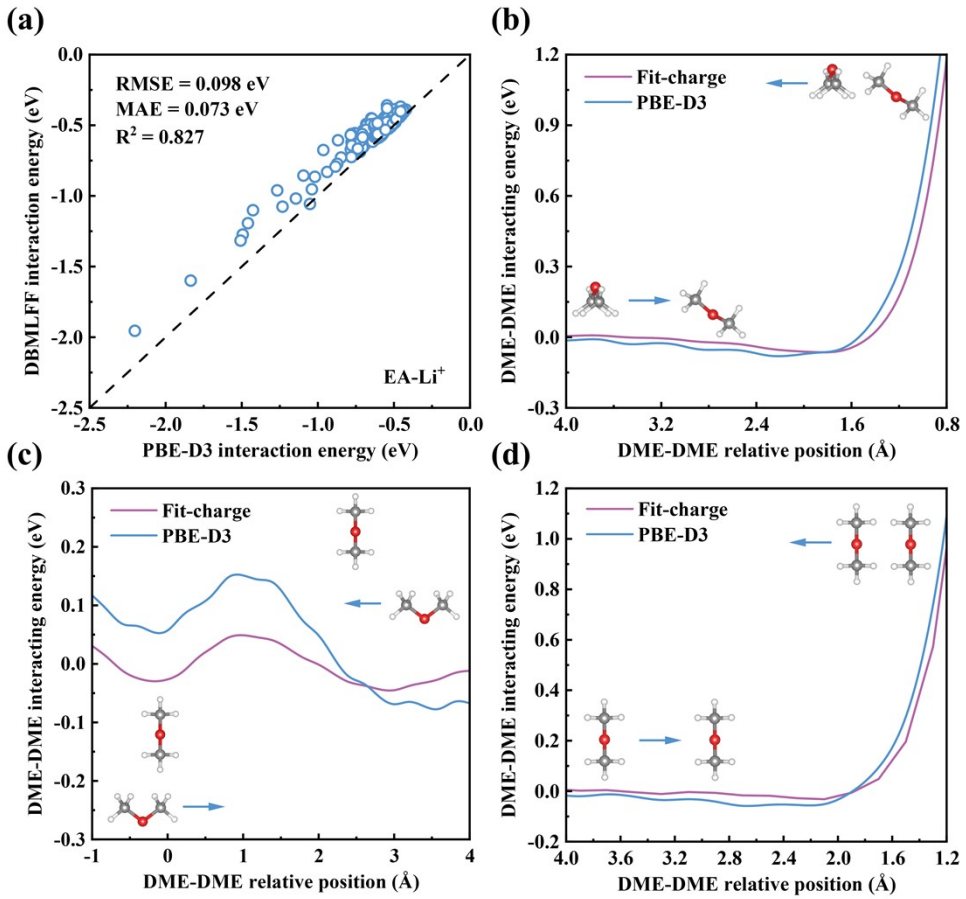

Fig. S9 (a) Comparison of intermolecular interaction energies for the EA-Li^+ system between the DBMLFF model and DFT (PBE-D3) calculations, with random molecular displacements and orientations. (c)-(d) Comparison of DME-DME intermolecular interaction energies between the DBMLFF model and DFT (PBE-D3) for three representative configurations.

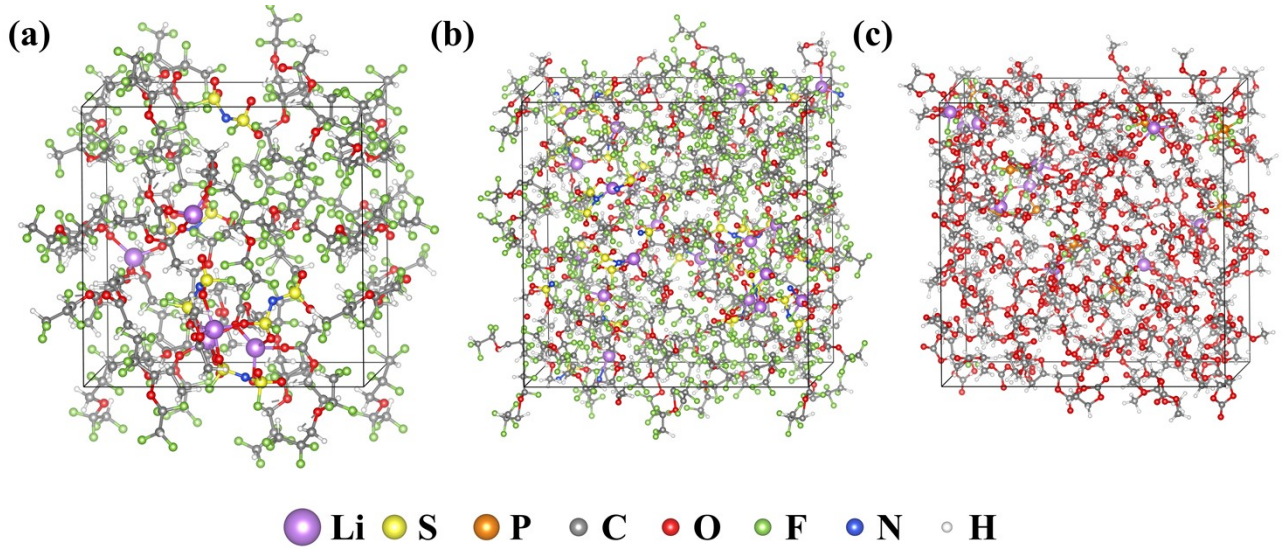

Fig. S10 Structural snapshots of (a) the LiFSI/EA/TTE system, (b) the LiFSI/EGDME/TTE system, and (c) the $LiPF_6$/EC/DMC system.

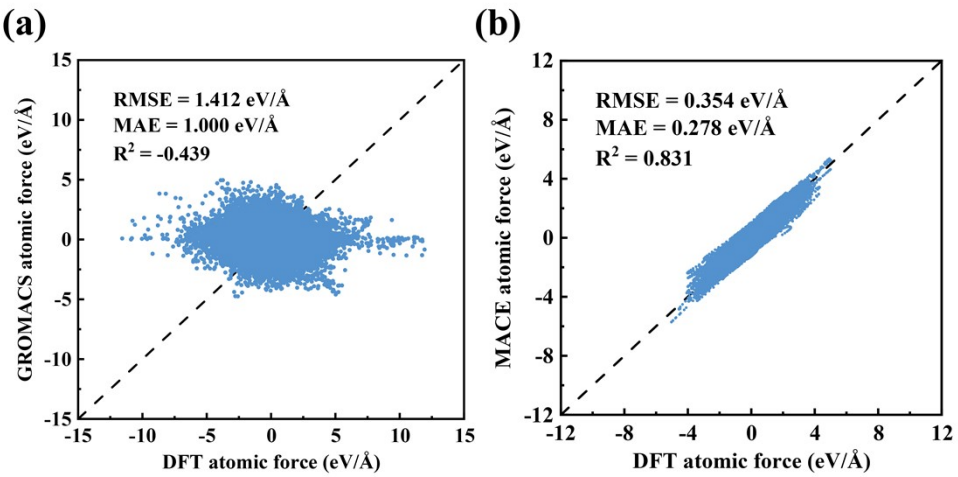

Fig. S11 Benchmarking of simulated atomic forces against DFT for a 460-atom LiFSI/EA/TTE electrolyte system. (a) GROMACS. (b) MACE.

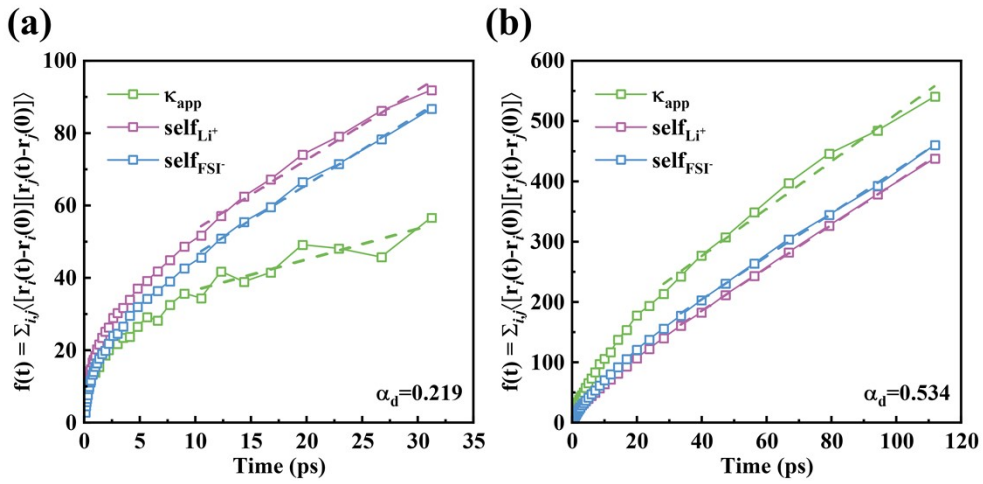

Fig. S12 Compute α(t) using the initial 4% segment of the MD trajectory for (a) LiFSI/EGDME/TTE and (b) $LiPF_6$/EC/DMC electrolyte systems. Here, κ_{app} is the time correlation function for collective ion conduction; $self_{Li^+}$ and $self_{FSI^-}$ denote the self-diffusion correlation functions for Li^+ and FSI^-, respectively.

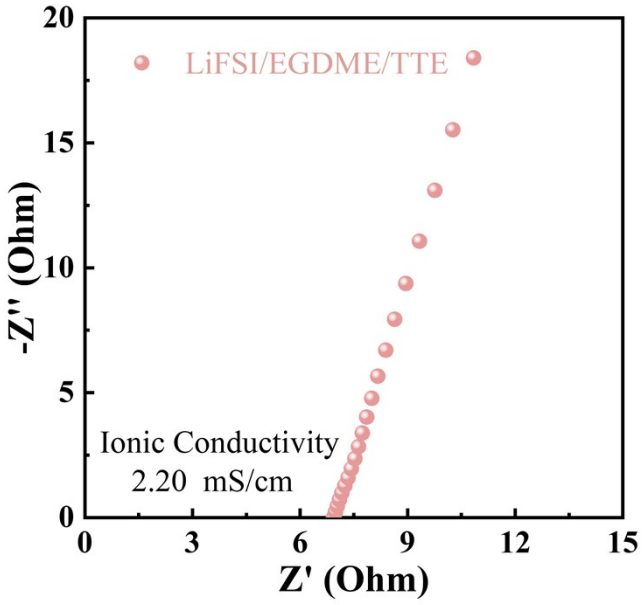

Fig. S13 Nyquist plot of the LiFSI/EGDME/TTE electrolyte system, showing an ionic conductivity of 2.20 mS/cm.

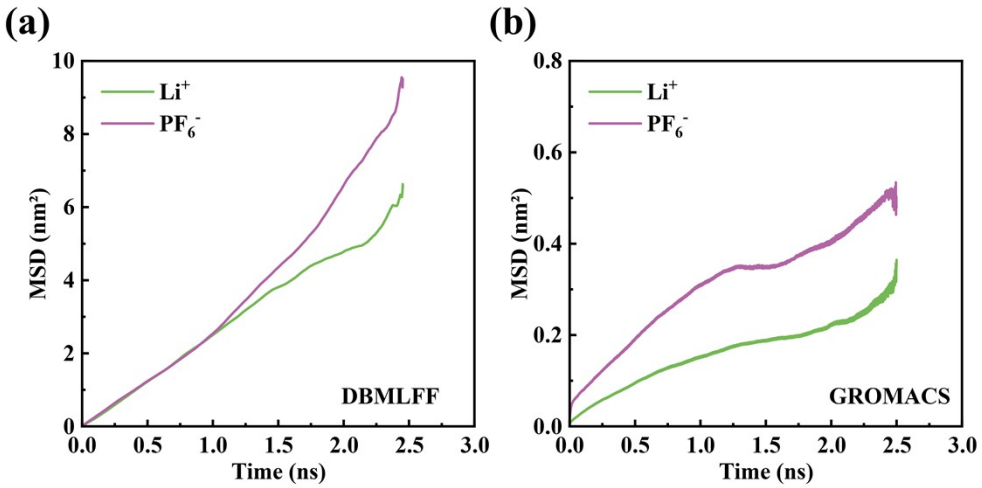

Fig. S14 Mean square displacement (MSD) of Li^+ and PF_6^- in the $LiPF_6$/EC/DMC system from (a) DBMLFF and (b) GROMACS simulations.

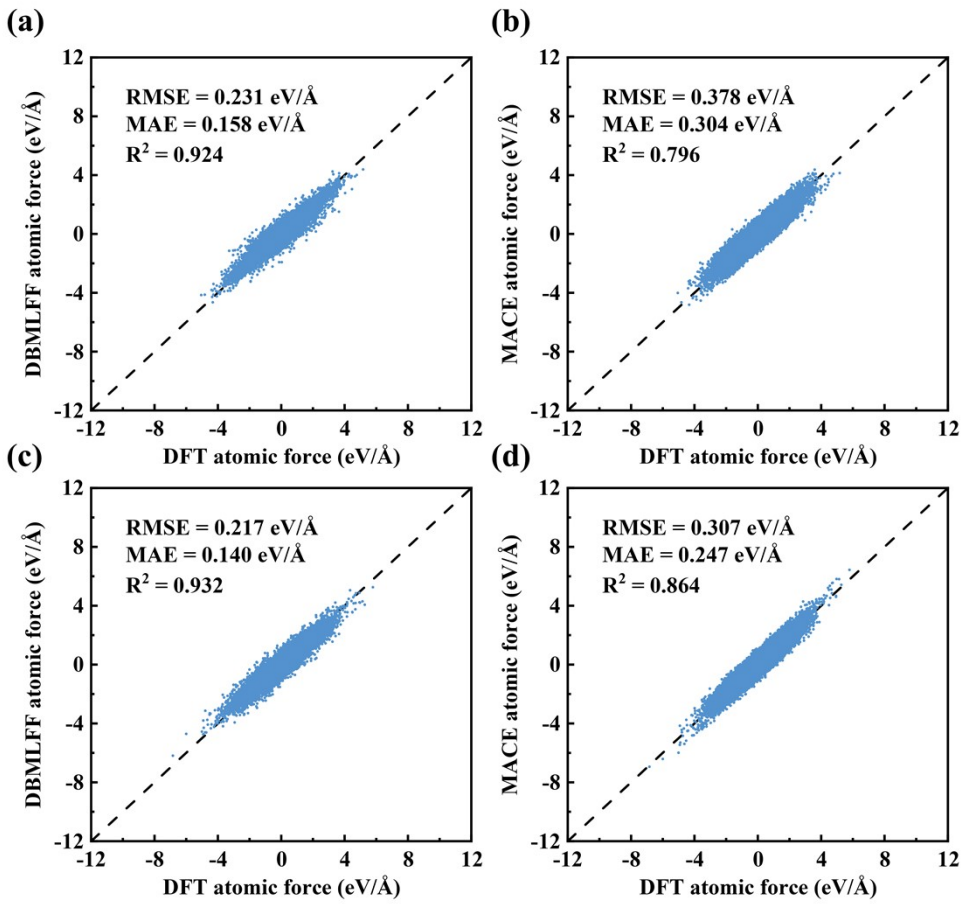

Fig. S15 Benchmarking of ML-predicted atomic forces against reference DFT calculations. (a, b) Forces in the LiFSI/EGDME/TTE system predicted by (a) the DBMLFF and (b) the MACE model. (c, d) Forces in the $LiPF_6$/EC/DMC system predicted by (c) the DBMLFF and (d) the MACE model.

Table S1. Diffusion coefficients and ionic conductivities (κ) in the LiFSI/EGDME/TTE system, determined using various techniques.

Methods	D_{Li^+} (10^{-10} m^2 s^{-1})	D_{FSI^-} (10^{-10} m^2 s^{-1})	κ (mS cm^{-1})
GROMACS	0.486	0.704	1.511
DBMLFF	0.849	1.030	2.386
Experiments	1.377	1.180	2.200

Table S2. Diffusion coefficients and ionic conductivities (κ) in the $LiPF_6$/EC/DMC system, determined using various techniques.

Methods	D_{Li^+} (10^{-10} m^2 s^{-1})	D_{PF6^-} (10^{-10} m^2 s^{-1})	κ (mS cm^{-1})
GROMACS	0.211	0.422	1.393
DBMLFF	3.581	4.205	13.800
Experiments	1.8	2.7	11.2

Table S3. Enthalpies of vaporization of different substances at 298 K and 1 atm.

Molecule	GROMACS ($kJ \cdot mol^{-1}$)		DBMLFF ($kJ \cdot mol^{-1}$)		Experiments ($kJ \cdot mol^{-1}$)
	Mean	SE	Mean	SE	
DME	26.37	0.01	23.40	0.03	21.2[1]
EA	53.87	0.03	38.91	0.02	35.69[2]
TTE	44.79	0.05	36.21	0.09	40.2[3]
EGDME	50.08	0.39	38.36	0.06	36.76[4]
DMC	62.92	0.02	43.75	0.09	37.70[5]

References

1 R. M. Stephenson and S. Malanowski, *Handbook of the Thermodynamics of Organic Compounds*, 1987.

2 V. Majer, V. Svoboda and H. V. Kehiaian, 1985.

3 J. Murata, S. Yamashita, M. Akiyama, S. Katayama, T. Hiaki and A. Sekiya, *J. Chem. Eng. Data*, 2002, **47**, 911–915.

4 D. Li, W. Fang, W. Xie, Y. Xing, Y. Guo and R. Lin, *Energy Fuels*, 2009, **23**, 794–798.

5 W. V. Steele, R. D. Chirico, S. E. Knipmeyer and A. Nguyen, *J. Chem. Eng. Data*, 1997, **42**, 1008–1020.